First-Principles Calculations of the Urbach Tail in the Optical Absorption Spectra of Silica Glass

B. Sadigh, P. Erhart, D. Åberg, A. Trave, E. Schwegler, and J. Bude

Lawrence Livermore National Laboratory, Chemistry, Materials and Life Sciences Directorate, Livermore, California 94550, USA
(Received 20 July 2010; published 10 January 2011)

We present density-functional theory calculations of the optical absorption spectra of silica glass for temperatures up to 2400 K. The calculated spectra exhibit exponential tails near the fundamental absorption edge that follow the Urbach rule in good agreement with experiments. We discuss the accuracy of our results by comparing to hybrid exchange correlation functionals. We show that the Urbach rule holds in a frequency interval where optical absorption is Poisson distributed with very large statistical fluctuations. In this regime, a direct relation between the optical absorption coefficient and electronic density of states is derived, which provides a link between photoemission and absorption spectra and is used to determine the lower bound to the Urbach frequency regime.

At finite temperatures absorption spectra of insulators exhibit an exponential energy dependence near the fundamental absorption edge that varies with temperature according to [1]

$$\bar{\alpha}(\omega, T) = \alpha_0 \exp\left[-\sigma \frac{\hbar\omega_0(T) - \hbar\omega}{kT}\right]. \quad (1)$$

Here $\omega_0(T)$ is a linear function of temperature, which at 0 K is defined to be the optical gap, while σ and α_0 are constants that can be extracted from experiments. The Urbach rule, Eq. (1), has been observed universally in crystals as well as glasses. Extensive research over many decades [2] has shown that it arises from transitions between localized electronic levels resulting from band-edge fluctuations and extended states [3,4]. In a pioneering work on amorphous Si, the fluctuations in the single-particle energies at the band edges obtained from *ab initio* molecular-dynamics (MD) simulations in the local density approximation were found to be in good agreement with experimentally measured band tail widths [5]. Yet the question remains whether single-particle theories can provide a quantitative description of the Urbach tail in wide band gap materials. On the one hand, it has been shown that charge localization due to excitonic binding is responsible for the low-energy absorption peaks in these systems [6,7]. On the other hand, at elevated temperatures the phonon-induced localization of the single-particle states may very well be sufficient to provide a quantitative description of the observed exponential tails in optical spectra. In this Letter, we address this issue by investigating the Urbach rule in defect-free silica glass using *ab initio* MD simulations. A detailed comparison with experiments shows that the Urbach behavior can be accurately described within a single-particle picture for this system.

The present work has been motivated by the need to develop a better understanding of the process of laser damage to silica optics. Recently, the role of temperature

has been emphasized by experiments where damage was generated far below the bulk material threshold by photons of energy 3.55 eV at about $T_c = 2200$ K [8]. The thermal runaway at T_c is a direct result of the exponential temperature dependence of absorption in Eq. (1) [8]. However, extrapolation of experimental spectra [9] predicts a T_c that is several hundred kelvins higher than the measured value. The objective of this Letter is to study the physical processes that lead to absorption in a temperature and energy range for which experiments are not available. The key finding is that in the Urbach regime absorption is best described as a Poisson process of localized bursts that occur at subterahertz frequencies.

The MD simulations presented in this work are performed within the generalized gradient approximation (GGA) using the Perdew-Wang 1991 (PW91) parametrization [10,11] as implemented in the Vienna ab-initio simulation package [12] using the projector augmented wave method [13]. Calculations involve supercells containing 24 SiO_2 formula units, and the Brillouin zone is sampled by a $2 \times 2 \times 2$ Monkhorst-Pack k-point grid. In order to obtain a realistic glass model, we started from a liquid silica model obtained previously [14], which was quenched down to 0 K over a period of about 10 ps. The examination of the electronic structure of the resulting configurations revealed defect states due to the presence of stretched and broken bonds [15]. The defect states were eliminated from the model by optimization via a bond-switching Monte Carlo technique [16,17]. Several configurations were thus generated, each representing a random network with fixed bond lengths and angles. Subsequently, the configurations were structurally relaxed to the local GGA total energy minimum. The electronic density of states (DOS) of the final glass model is shown in Fig. 1(a) in comparison with Perdew's hybrid scheme using Perdew-Burke-Ernzerhof exchange and correlation functionals (PBE0) [18,19]. The GGA DOS includes a band gap shift of $\Delta_g = 2.6$ eV to account for the systematic

underestimation of the band gap. We find excellent agreement between the two calculations for the perfect glass. As a further test, we have explicitly compared the time evolution of the band-edge states and the total energy at 2200 K, calculated from GGA with PBE0 [20] calculations [Fig. 1(b)]. It appears that with a constant band gap shift of 2.6 eV, all calculations can be brought in agreement with each other. A similar conclusion was reached in studying point defects [21].

The absorption coefficient for photons of energy $\hbar\omega$ of an atomic configuration X can be calculated as follows:

$$\alpha(\omega; X) = \sqrt{2}\frac{\omega}{c}\sqrt{|\epsilon(\omega; X)| - \epsilon_R(\omega; X)}, \quad (2)$$

where $\epsilon(\omega; X)$ is the complex dielectric function $\epsilon = \epsilon_R + i\epsilon_I$. In the velocity gauge, ϵ_I can be directly computed from the single-particle wave functions and energies [22,23] as well as their occupancies f_{nk} as follows:

$$\epsilon_I(\omega; X) = \frac{4\pi^2 e^2}{m_e^2 \omega^2}\sum_{n,n'}(f_{n'k} - f_{nk})|M_{nn'}^k(X)|^2 \times \delta(\Delta_g$$
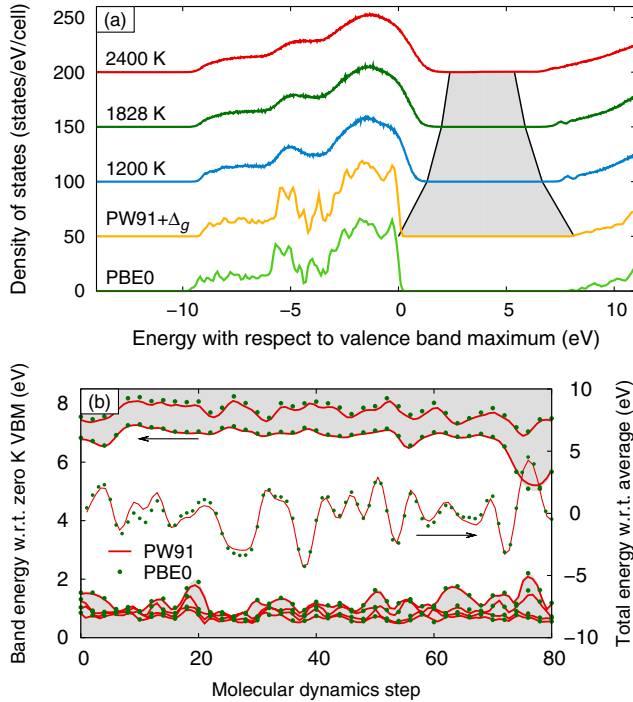$$+ e_{n'k}(X) - e_{nk}(X) - \hbar\omega), \quad (3)$$

FIG. 1 (color online). (a) DOS of the perfect glass at 0 K calculated by using the PBE0 hybrid functional and the PW91 functional with scissors correction (PW91 + Δ_g). Also shown is the DOS obtained from MD simulations at three different temperatures by using PW91 + Δ_g. (b) Single-particle energies of the four topmost valence band states and the two lowermost conduction band states (thick lines, large circles) as well as the total energy (thin lines, small circles) along an MD trajectory (generated by using PW91) are shown as obtained from the PBE0 hybrid functional compared with the PW91 + Δ_g.

where $M_{nn'}^k(X)$ are the polarization-averaged dipole matrix elements between the states nk in the valence band and $n'k$ in the conduction band. The summations in Eq. (3) run over bands and spins, and the real part ϵ_R can be obtained from ϵ_I through a Kramers-Kronig relation. Since the latter involves an integration over the entire frequency spectrum, we have included as many as 1000 unoccupied bands in our calculations.

At finite temperatures, the response functions as well as the DOS are calculated by classical ensemble averaging over ionic displacements in the Born-Oppenheimer approximation, treating the electronic transitions as instantaneous. Figure 1(a) shows the average DOS at three different temperatures. The gray region depicts the narrowing of the band gap with increasing temperature, leading to an exponential increase of the free carrier densities. While at 2400 K the density of free carriers can be as large as 10^{17} cm^{-3}, it is still too small to have any measurable impact on the absorption in the Urbach regime.

The DOS can be linked to optical absorption via the joint density of states (JDOS), which at 0 K is defined as $J(\omega) = \int\rho_v(\omega')\rho_c(\omega' + \omega)d\omega'$, where $\rho_{v(c)}(\omega)$ is the DOS of the valence (conduction) bands. At finite temperatures, a direct relationship between the JDOS and the DOS exists only if the fluctuations in the valence and the conduction bands are independent:

$$\langle\mathcal{J}(\omega)\rangle_T \approx \int\langle\rho_v(\omega')\rangle_T\langle\rho_c(\omega' + \omega)\rangle_T d\omega'. \quad (4)$$

We find that the above is a very good approximation over the entire frequency range, which implies that knowledge of the DOS is sufficient to determine of the JDOS. In the Urbach regime, the JDOS can be linked to the dielectric function via

$$\langle\epsilon_I(\omega)\rangle_T \approx \bar{\mu}(T)\langle\mathcal{J}(\omega)\rangle_T. \quad (5)$$

This is illustrated in Fig. 2(a), where the low-frequency exponential tail of the dielectric function and the JDOS are shown to coincide when the latter is scaled by a temperature-dependent effective dipole transition probability $\bar{\mu}(T)$. This result suggests that the frequency dependence of the Urbach tail originates from the exponential decay of the JDOS, while the matrix elements provide an effective temperature-dependent prefactor. As shown in the inset in Fig. 2(a), $1/\bar{\mu}(T)$ decreases linearly with temperature, resulting in a reduction by a factor of 2 between 1200 and 2400 K. As was noted by Chang, Rohlfing, and Louie [7], the inclusion of excitonic effects has a small impact on the JDOS. They mainly alter the oscillator strength of transitions to correlated electron-hole states, which may modify the prefactor $\bar{\mu}(T)$ but not the overall shape of the Urbach tail.

After obtaining the dielectric functions at different temperatures, it is straightforward to calculate the absorption spectra shown in Fig. 2(b) via Eq. (2). Fitting the exponential tails of these spectra to Eq. (1) yields a linear

temperature dependence for $\omega_0(T)$ as shown in the inset in Fig. 2(b), extending the Urbach rule to 2400 K. The fit also gives $\sigma = 0.473$, in fair agreement with the experimental value of $\sigma = 0.585$ [9]. The Tauc gap, which is the threshold energy for the onset of extended-to-extended electronic transitions, can be extracted as well. Following Ref. [9], where the Tauc gap was defined as the photon energy corresponding to 5×10^3 cm^{-1} absorption, one obtains the data shown in the inset in Fig. 2(b), again demonstrating excellent agreement.

The good agreement between the calculated and experimental Tauc gaps is the most definite evidence that a single-particle picture is sufficient for describing optical absorption in the Urbach regime. Since excitonic effects lead to increased absorption at low energies, our calculated Tauc gaps would have been significantly higher than experiment if electron-hole interactions were essential. In the Urbach regime the ratio $\langle \epsilon_I(\omega) \rangle_T / \langle \epsilon_R(\omega) \rangle_T \ll 1$. A first-order Taylor expansion of Eq. (2) with respect to this quantity in conjunction with Eq. (5) yields a direct relation between the absorption coefficient and the JDOS:

$$\langle \alpha(\omega) \rangle_T \approx \frac{\omega}{c} \frac{\langle \epsilon_I(\omega) \rangle_T}{\sqrt{\langle \epsilon_R(\omega) \rangle_T}} \approx \frac{\omega}{c} \frac{\bar{\mu}(T)}{\sqrt{\langle \epsilon_R(0) \rangle_T}} \langle \mathcal{J}(\omega) \rangle_T. \quad (6)$$

The above equation together with Eq. (4) establishes a link between the absorption coefficient and the DOS in the

vicinity of the absorption edge, where the temperature dependence of the prefactor mainly enters through $\bar{\mu}(T)$, while $\langle \epsilon_R(0) \rangle_T$ varies only weakly with temperature, i.e., from 1.81 at 0 K to 1.99 at 2400 K. This result provides a connection between photoemission and optical absorption experiments in the Urbach regime.

We now discuss fluctuations in the optical absorption due to atomic vibrations. A lower bound can be obtained by using Eq. (6) and considering only fluctuations in the JDOS. Figure 3(a) shows unexpectedly large fluctuations in the JDOS in the Urbach regime with the ratio
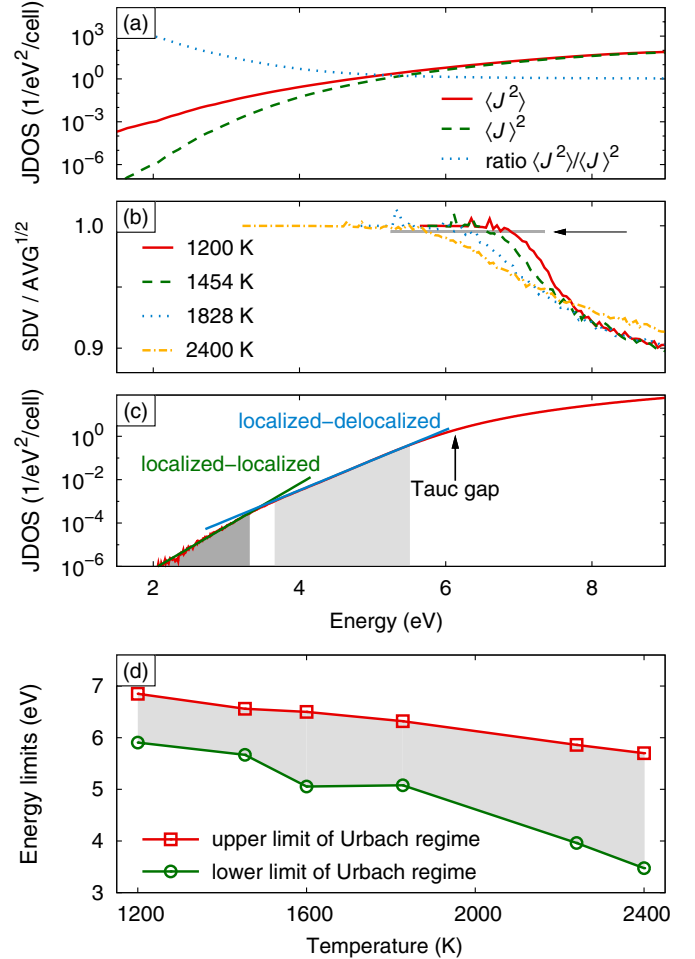
FIG. 3 (color online). (a) First and second moments of the JDOS as well as their ratio at 2400 K. (b) In the Urbach regime the standard deviation of the JDOS equals the square root of the average indicative of a Poisson distribution. The energy at which the ratio deviates from one (indicated by the arrow) provides a simple measure for the upper limit of the Urbach regime. (c) At low energies the JDOS exhibits two distinct regions corresponding to localized-delocalized (Urbach regime) and localized-localized transitions. Each region is described by a different exponential whose crossing point defines a lower limit for the Urbach regime. Note that the Tauc gap lies above the region in which the JDOS exhibits exponential tails. (d) Upper and lower limits of the Urbach regime extracted from the data presented in (b) and (c).
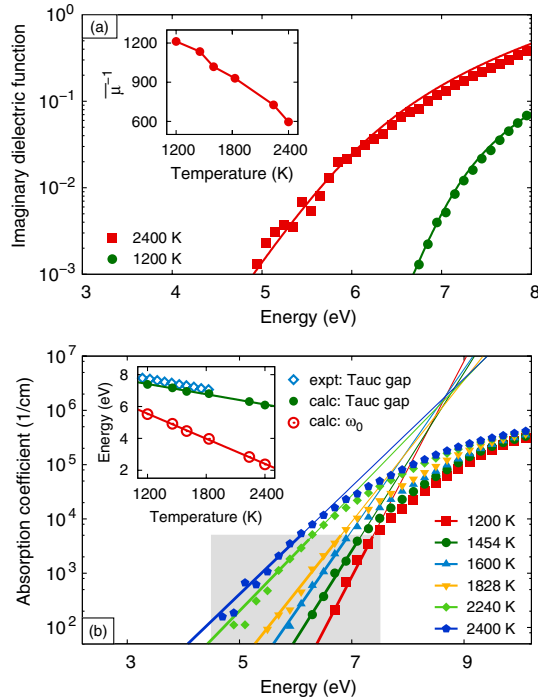

FIG. 2 (color online). (a) JDOS rescaled by $\bar{\mu}(T)$ (solid lines) and imaginary dielectric function (symbols). The inset shows $\bar{\mu}(T)^{-1}$ as a function of temperature. (b) Absorption coefficient in the Urbach regime calculated by using PW91 + Δ_g. The inset shows the result of a fit to Eq. (1) and the comparison with the experimental data from Saito and Ikushima [9]. The shaded region depicts the Urbach regime.

$\langle \mathcal{J}^2(\omega)\rangle_T / \langle \mathcal{J}(\omega)\rangle_T^2$ reaching 10^4. Hence the standard deviation from mean absorption in the Urbach tail can be up to 2 orders of magnitude larger than $\langle \alpha(\omega)\rangle_T$.

The large fluctuations in the Urbach regime originate from the discrete nature of the JDOS itself. Even if $\langle \mathcal{J}(\omega)\rangle_T \ll 1$, there can exist only an integer number $\mathcal{N}$ of pairs of electronic states available for transition at any instant of time. Hence the absorption coefficient locally varies between 0 and $\bar{\mu}^2 \times \mathcal{N}$, which can amount to fluctuations much larger than the mean value $\langle \mathcal{J}\rangle_T$ itself. This is a direct consequence of the quantum nature of matter. Let us define an absorption event as the instant of time when $\mathcal{N} > 0$. Whenever absorption events occur rarely enough to be considered independent, the absorption process is Poisson distributed with $\langle \mathcal{J}(\omega)\rangle_T$ interpreted as the average rate of occurrence. An important signature of the Poisson distribution is that its standard deviation is equal to the square root of its average. As shown in Fig. 3(b) in the Urbach regime, this is indeed the case with the ratio sharply decreasing for higher energies. The abrupt transition provides a natural definition for the upper bound to the Urbach region ω_U. Figure 3(d) shows that, in the temperature range considered here, ω_U decreases linearly. These observations bestow the finite-temperature JDOS in the Urbach tail with distinct physical significance as it represents the average rate of occurrence of absorption events in this frequency interval.

We can also determine the lower bound to the Urbach frequency domain by using Eq. (4) to compute $\langle \mathcal{J}(\omega)\rangle_T$ down to very small values with good statistical accuracy. Figure 3(c) shows that at very low energies the slope of the signature exponential decay of the Urbach tail changes. The frequency ω_L at which this transition occurs can be used to identify the lower bound of the Urbach regime, the temperature dependence of which is shown in Fig. 3(d). This lower-frequency region corresponds to transitions between localized levels in the exponential tails of the valence and the conduction bands, while the Urbach tail originates from transitions between localized tail states and extended bandlike states.

Finally, let us discuss modeling laser heating in silica which can be described by a heat conduction equation with a source term. The latter incorporates energy deposition by linear coupling to laser light, $\bar{\alpha}(\omega, T)I(\mathbf{r})$, where $I(\mathbf{r})$ is the laser light intensity. Neglecting fluctuations, this term can be parametrized by $\bar{\alpha}(\omega, T) = \langle \alpha(\omega)\rangle_T$. However, the rare event nature of absorption in the Urbach regime calls for $\bar{\alpha}(\omega, T)$ to be treated as a discrete Poisson process, where at a rate proportional to $\langle \mathcal{J}(\omega)\rangle_T$ an absorption event of strength $\omega \bar{\mu}^2 / c \sqrt{\langle \epsilon_R(0)\rangle_T}$ takes place. The large fluctuations introduced in this way can reduce the predicted thermal runaway temperature leading to better agreement with experiments.

[1] F. Urbach, Phys. Rev. **92**, 1324 (1953).
[2] T. H. Keil, Phys. Rev. **144**, 582 (1966); C. M. Soukoulis, M. H. Cohen, and E. N. Economou, Phys. Rev. Lett. **53**, 616 (1984); B. I. Halperin and M. Lax, Phys. Rev. **148**, 722 (1966).
[3] T. A. Abtew and D. A. Drabold, Phys. Rev. B **75**, 045201 (2007).
[4] Y. Pan, F. Inam, M. Zhang, and D. A. Drabold, Phys. Rev. Lett. **100**, 206403 (2008).
[5] D. A. Drabold, P. A. Fedders, S. Klemm, and O. F. Sankey, Phys. Rev. Lett. **67**, 2179 (1991).
[6] L. X. Benedict and E. L. Shirley, Phys. Rev. B **59**, 5441 (1999).
[7] E. K. Chang, M. Rohlfing, and S. G. Louie, Phys. Rev. Lett. **85**, 2613 (2000).
[8] J. Bude, G. Guss, M. Matthews, and M. L. Spaeth, Proc. SPIE Int. Soc. Opt. Eng. **6720**, 672009 (2007).
[9] K. Saito and A. J. Ikushima, Phys. Rev. B **62**, 8584 (2000).
[10] J. P. Perdew and Y. Wang, Phys. Rev. B **33**, 8800 (1986).
[11] J. P. Perdew, in *Electronic Structure of Solids*, edited by P. Ziesche and H. Eschrig (Akademie Verlag, Berlin, 1991), p. 11.
[12] G. Kresse and J. Hafner, Phys. Rev. B **47**, 558 (1993); **49**, 14 251 (1994); G. Kresse and J. Furthmüller, *ibid.* **54**, 11 169 (1996); Comput. Mater. Sci. **6**, 15 (1996).
[13] P. E. Blöchl, Phys. Rev. B **50**, 17 953 (1994); G. Kresse and D. Joubert, *ibid.* **59**, 1758 (1999).
[14] A. Trave, P. Tangney, S. Scandolo, A. Pasquarello, and R. Car, Phys. Rev. Lett. **89**, 245504 (2002).
[15] G. Pacchioni and G. Ieranó, Phys. Rev. B **56**, 7304 (1997).
[16] T. Bakos, S. N. Rashkeev, and S. T. Pantelides, Phys. Rev. B **70**, 075203 (2004).
[17] F. Wooten, K. Winer, and D. Weaire, Phys. Rev. Lett. **54**, 1392 (1985).
[18] J. P. Perdew, K. Burke, and M. Ernzerhof, Phys. Rev. Lett. **77**, 3865 (1996); **78**, 1396(E) (1997).
[19] M. Ernzerhof, J. P. Perdew, and K. Burke, Int. J. Quantum Chem. **64**, 285 (1997); M. Ernzerhof and G. E. Scuseria, J. Chem. Phys. **110**, 5029 (1999); C. Adamo and V. Barone, *ibid.* **110**, 6158 (1999).
[20] J. Heyd, G. E. Scuseria, and M. Ernzerhof, J. Chem. Phys. **118**, 8207 (2003); **124**, 219906(E) (2006).
[21] A. Alkauskas, P. Broqvist, and A. Pasquarello, Phys. Rev. Lett. **101**, 046405 (2008).
[22] R. Del Sole and R. Girlanda, Phys. Rev. B **48**, 11 789 (1993).
[23] Z. H. Levine and D. C. Allan, Phys. Rev. B **43**, 4187 (1991).